The CleoSim Radar Simulator

Andrea Manzoni[1], Michele D'Amico[1], Fabio Milani[2] and Jean-Philippe Wasselin[3]

[1]*DEIB, Politecnico di Milano, Milano, Italy*
[2]*IDS Ingegneria dei Sistemi, Roma, Italy*
[3]*Rockwell Collins France, Blagnac, France*

(Dated: 24 July 2014)

Andrea Manzoni

1 Introduction

Civil and military transport aircraft are usually equipped with airborne weather radars (AWR), that implement various functionalities for the detection of dangerous weather phenomena. In principle, the highest detection performances can be obtained by the Doppler-polarimetric radars; in fact, polarimetric radars can provide more refined information on the type of precipitation once the model of specific hydrometeor (rain, snow or hail) is known. So far, polarimetry has been used in meteorological ground-based radars, but not in airborne commercial radars (apart from some experimental systems).

During the CLEOPATRA project a new airborne Doppler-polarimetric radar simulator was developed (CleoSim), that combines the description of the meteorological scenario at mesoscale level (typical of the environment simulators) with the capability of generating accurate time series of raw signals received by the sensor (typical of the microphysical simulators). The simulator generates a virtual meteorological environment, simulates the transmission of the electromagnetic pulses, and solves the monostatic radar equation to produce a stream of synthetic I&Q samples.

The main application of CleoSim is the generation of synthetic signals to perform extensive tests of the signal processing and trajectory optimization algorithms developed in the framework of another related project (KLEAN). Obviously, algorithm performance analysis results are strictly dependent on the reliability of the polarimetric radar simulator, that therefore needs to be thoroughly validated.

In this contribution we present the results of the validation phase of CleoSim; the simulator was validated by comparing synthetic data against both "textbook" scenarios and measured data; those last were gathered concurrently by two ground-based Doppler-polarimetric radars (operating at C and X band) owned and operated by ARPAP (Agenzia Regionale per la Protezione dell'Ambiente del Piemonte) during an ad-hoc experimental campaign, conducted in the course of the Cleopatra project.

2 Airborne Radar

The current generation of airborne weather radars (AWR) uses flat-plate reflectors, composed of several slits fed in phase. This solution, in addition to have a lower cost, ensures a much more focused beam (about 3.5˚ measured at -3 dB) and small side lobes, reducing the impact of ground clutter. This reflector is placed on a 2D mechanism enabling independent rotations over azimuth (from -90˚ to 90˚) and elevation (from -45˚ to 45˚), allowing both PPI that RHI scans.

The airborne radar systems mounted on civil aircrafts operate mainly in X-band (9.3 GHz), a tradeoff among signal attenuation, echoes accuracy and lack of space onboard. Moreover, the most advanced AWRs can exploit different processing techniques, such as the pulse compression and the ground clutter rejection. In fact, although the radar beamwidth is narrow enough, the ground reflectors are so strong (especially cities) that the ground clutter is measured far out of the radar beam, over an angle of 8˚.

The newest airborne radars can detect the presence of wind shear, an event in which the wind abruptly changes its speed or direction (or both) over a small distance, extremely dangerous during aircraft landing. So these cutting-edge AWRs can be considered Doppler radars with some limitations. On the contrary, it has not been observed commercially the presence of polarimetric AWRs, leaving all the benefits provided from this upgrade.

3 The CleoSim Simulator recap

In order to fill this gap a new airborne Doppler and polarimetric radar simulator has been developed during the CLEOPATRA project; the simulator was named CleoSim, from Cleopatra Simulator. It appears of great interest the availability of a sophisticated AWR simulator that is capable of discriminating the effect of different hydrometeors contributions on the echo received by the radar. In particular, it is very useful to evaluate the impact that microphysical models changes as well as sensor properties variations have on the received signals.

The CLEOPATRA project falls within the Clean Sky program, a European Joint Technology Initiative (JTI) aiming at rethinking the aviation industry with the addition of many green technologies. The goal of the Cleopatra project was to design an airborne radar simulator which could compute the radar I&Q signals, employed for the definition of advanced algorithms for weather detection (WXR) needed to optimize the air routes and enrich the current flight simulators with new features. Clearly, the success of these weather detection algorithms is conditioned on the proper functioning of CleoSim, which has to calculate I&Q signals consistent with the simulated meteorological scenario. For this reason it was essential to carry out a careful validation of the simulator.

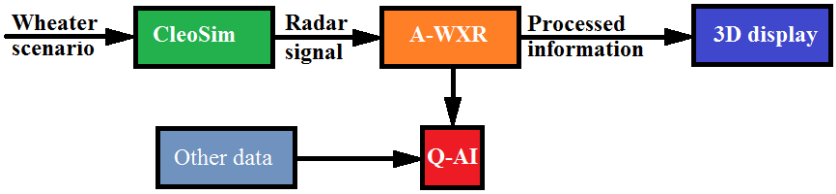

Figure 1: Cleoparta project exploitations.

CleoSim is a simulator that aims at defining a new class of radar simulation, combining the description of the meteorological scenario at mesoscale level (a feature typical of the environment simulators) with the ability to generate accurate time series of I&Q signals (a characteristic of the microphysical simulators) for any polarization scheme (Capsoni et al., 2001). So, we could describe CleoSim as a microphysical polarimetric and Doppler airborne weather radar simulator that simulates the transmission of electromagnetic pulses solving the monostatic radar equations (Battan, 1973) over a large synthetic meteorological scenario.

The simulator is made by three models that operate in cascade. The first model to be called is the meteorological one, where the user selects a mesoscale meteorological file (.GRIB), containing some events of interest. Among these events are included either potentially dangerous situations to the safety of the aircraft or not threatening situations that still have an impact on the onboard performances. The meteorological model turns the meteorological file into a three-dimensional grid where each point (voxel) of the volume is described by 15 parameters, e.g. the temperature, pressure, integral quantities of the different hydrometeors, etc. This grid consists of 60 vertical levels and provides a horizontal resolution of 2.5 km, which can be refined to 0.5 km in case of promising events.

The radar model is activated for the first time with the A procedure (RMAP), that calculates the WORs (Weather Observation Regions) and the CORs (Clutter Observation Regions), namely the regions that during the transmission of a pulse are illuminated by the beamwidth and intersect hydrometeors and ground clutter, respectively. Because of the antenna rotation and aircraft displacement along the route, the WOR and the COR differ for each pulse. During this procedure the user can define the coordinates of the plane, its route, the parameters of the sensor and the scanning strategy. Moreover, it's possible to select various customizations, such as the pulse compression (chirping or phase coding) and the modeling of clutter (specifying the elevation profile for different surfaces), etc. Once the WORs and the CORs are calculated, they are used to filter the meteorological data, to reduce the computational complexity of the subsequent operations.

The electromagnetic model takes as input the meteorological grid and computes the scattering and absorption properties for the different types of hydrometeors. The scattering properties are needed to let CleoSim consider each particle as an independent scatterer, a fundamental step to preserve the phase relationships between the signals that form the received echo. The forward and backward scattering amplitudes are calculated independently for each type of hydrometeors, which is described through some microphysical models (for the DSD, the terminal fall velocity, the particles shape, etc.). The scattering amplitudes for rain and for all distorted hydrometeors (except ice crystals that fulfil that Rayleigh condition) are computed using a point-matching technique (Oguchi, 1983).

Finally, the radar model is enabled again to perform the B procedure (RMBP), designated to the calculation of a time series of I&Q signals. The RMBP fills randomly the WORs with one or more populations of particles, whose microphysical description is retrieved from the EM model. Since it is not feasible to numerically reproduce an entire population nor to maintain the correct relationship between different diameters, a compression algorithm of the population is implemented, in order to generate a limited number of synthetic drops without altering the scattering proper of a real population. The algorithm sets for each type of hydrometeor (rain, snow, hail, melting layer, ice, etc.) a finite number of classes of diameters and a maximum number of synthetic drops for each class (for the rain a good tradeoff is done by 300 classes with 5 drops each). The RMBP is also in charge of updating the position of the drops between one pulse and the next, due to the fall velocity, winds and turbulences. Then, for each pulse and independently for each polarization are calculated the I&Q signals by solving the monostatic radar equations. Eventually, the background noise and the attenuation caused by the different precipitation are added (it's also possible to turn artificially off the attenuation).

4 CleoSim validation over analytic environments

Firstly, the validation of the simulator has been conducted over analytical scenarios, used to reproduce textbook cases. The choice of operating in well-known meteorological environments allows a detailed comparison between the results produced by the CleoSim and those expected from radar meteorological theory. The simulations were carried out mainly over scenarios with uniform rain, to know without any ambiguity the origin if the echoes. Over these meteorological environment both RHI and PPI scans were performed, the latter in the two reference cases (vertical and frontal pointing angle).

As an example in Fig. 2 are shown the main radar measurables obtained for a PPI scan with frontal pointing performed in a meteorological scenario with uniform rain (with a rain rate R of 10 mm/h). The number of transmitted pulses is 512, with a polarization alternating scheme (H-V), a PRF of 1000 Hz and a pulse width (PW) of 10 µs.

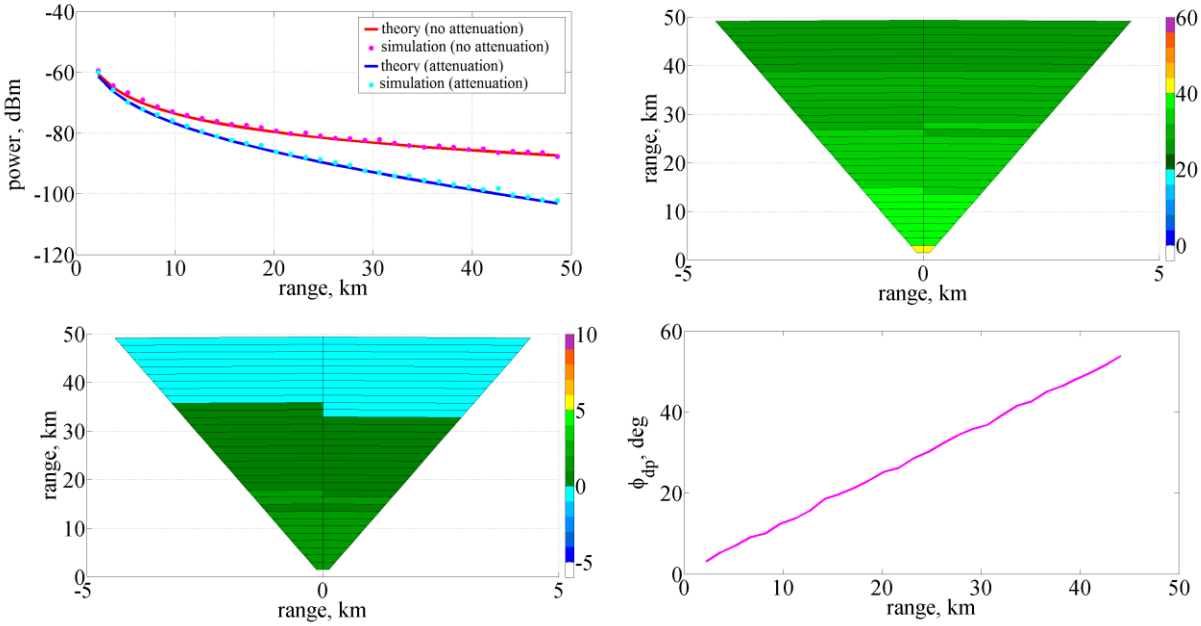

Figure 2: Received power, reflectivity, differential reflectivity and differential phase shift for an analytic scenario with uniform rain with R=10 mm/h and frontal pointing angle.

The comparison between simulated and theoretical results is shown in Fig. 2 for the received power, while for the other radar measurables is reported in Tab. 1, where the numbers are related at the first radar cell (the closest to the antenna).

Table 1: Comparison between simulated and theoretical values for Z, Z_{DR} and K_{dp}.

Radar observable	Simulated values	Theoretical values
Z	40.08 dBZ	40.08 dBZ
Z_{DR}	1.64 dB	1.72 dB
K_{dp}	0.79˚/km	1.18˚/km

Obviously, the fluctuations shown in Fig 2 are due to the fact that the scenario is dynamic, then for each transmitted pulse there is a different combination of the signal phases backscattered by the particles into the resolution volume. For this reason was useful to study the evolution of the standard deviation of Z against (i) the number of pulses averaged per block, (ii) the range from the radar and (iii) the PRF. The trend of σ is presented in Fig. 3 for a simulation with vertical pointing over a uniform rain with R = 6 mm/h. Fig. 3a shows a good level of agreement with the theory (orange curve), as well as the Fig. 3b which excludes any dependence on the range for the estimation of Z. Then, Fig. 3c shows an increase of the standard deviation as the PRF grows, as the scenario observed by the radar between two consecutive pulses remains more correlated.

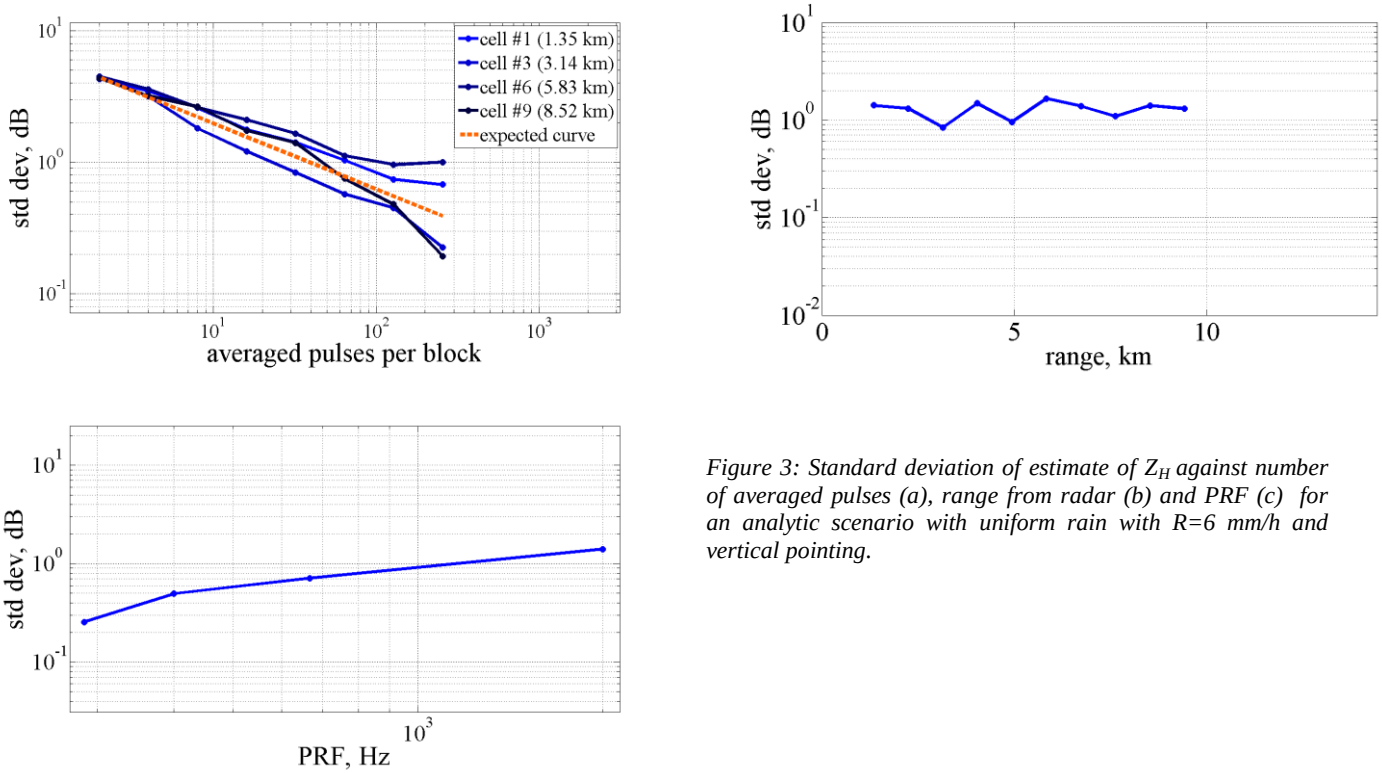

Figure 3: Standard deviation of estimate of Z_H against number of averaged pulses (a), range from radar (b) and PRF (c) for an analytic scenario with uniform rain with R=6 mm/h and vertical pointing.

For the two reference cases (vertical and frontal pointing angle) were also evaluated some statistical and spectral properties of the signal generated by the simulator (D'Amico, 1999). Among these properties was calculated the autocovariance of the linear power as a function the pulse lag. This function is closely linked to the power spectral density, being each of them the Fourier (anti)transform of the other. As expected, for vertical pointing we found a Doppler spectrum (Fig. 4, on the top) which represents the raindrops terminal velocity spectrum and is very similar to the theoretical spectra present in the literature (Doviak and Zrnić, 1993). In this case the autocovariance decays to values lower than 1/e after a time interval of only 4 pulses (2 ms), showing that the scenario is rapidly variant. On the contrary, the frontal pointing (Fig. 4, on the bottom) has the dual situation, with a narrow Doppler spectrum that is centered on the zero (since the radar detects only the movements on the plane, which are zero since in the simulation we canceled all the wind components) and an autocovariance which shows an environment in slow evolution.

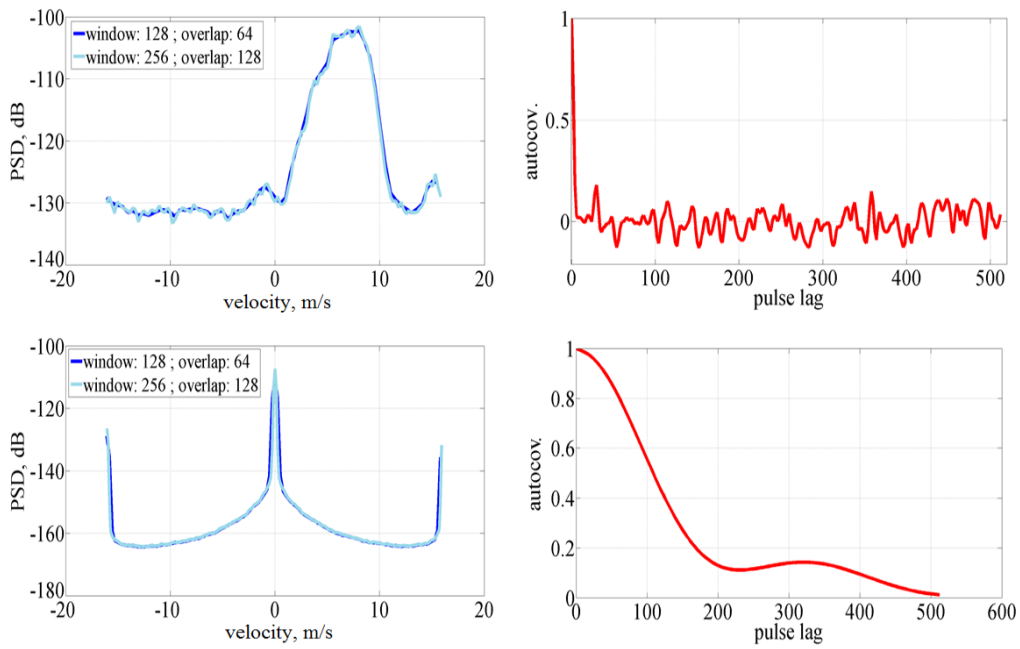

Figure 4: Power spectral density (left) and autocovariance of linear power against pulse lag (right). The two figures on the top refer to vertical pointing, while the two on the bottom to frontal pointing.

5 The experimental campaign

During the Cleopatra project an ad-hoc experimental campaign has been conducted to gather measured data by two ground-based Doppler-polarimetric weather radars (operating at C and X band) owned and operated by ARPAP (Agenzia Regionale per la Protezione dell'Ambiente del Piemonte). For both radars, placed in Bric della Croce (C-band), near Turin, and in Vercelli (X-band), the measured data have been recorded for five days between October 2012 and March 2013 (stratiform precipitation events). The two radars are 59 km distant and their unfolded maximum range is enough to provide a large area covered by both the radars, as seen in Fig. 5. The measurement gathered and scans performed are listed in Tab. 2.

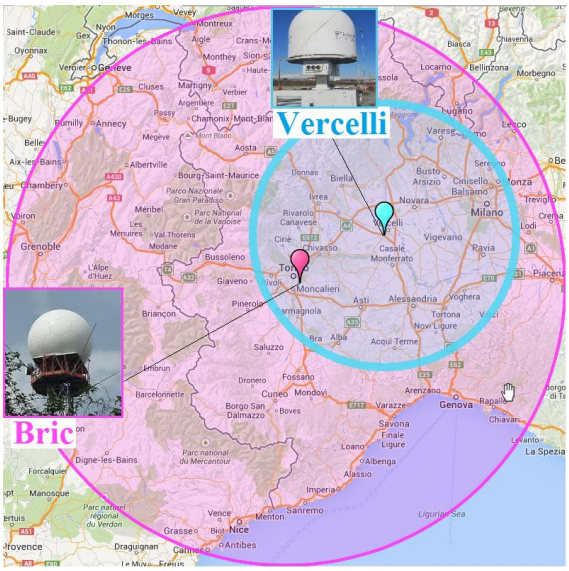

Figure 5: Coverage map for Bric della Croce and Vercelli weather radars.

Table 2: Scans and measured data collected during the measurement campaign by Bric and Vercelli radars.

Radar	Scan	Measured data
Bric	Volumetric (at 11 elev.)	Moments data (Z, Z_{DR}, V, ρ_{HV}, φ_{dp})
Vercelli	Volumetric (at 6 elev.) RHI (at 162° and 241°) puntamenti fissi	Moments data (Z, Z_{DR}, V, ρ_{HV}, φ_{dp}) I&Q data

The following pictures show the radar measurables collected on October 26, 2012 at 18:00 (UTC) by the WXR of Bric. The field of Z shows the most intense rain rate on the southwest of the map, with maximum values of 42 dBZ; the differential reflectivity has peaks over the same region (up to 4 dB), before dropping to negative values. While, from ρ_{HV} it's possible to distinguish the clutter from Alps (ρ_{HV}<0.7).

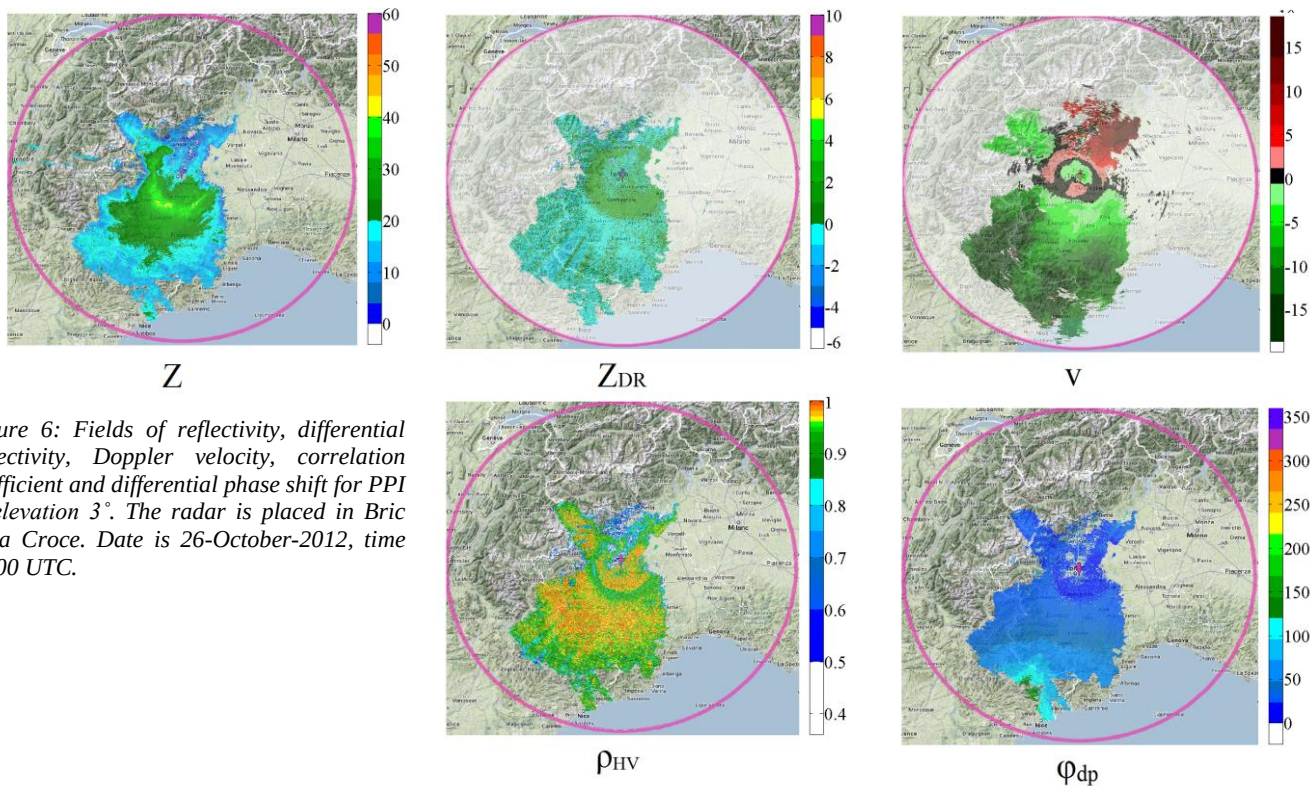

Figure 6: Fields of reflectivity, differential reflectivity, Doppler velocity, correlation coefficient and differential phase shift for PPI at elevation 3°. The radar is placed in Bric della Croce. Date is 26-October-2012, time 18:00 UTC.

6 CleoSim validation with measured data

The experimental observations acquired were then used and manipulated to validate the simulator. A validation is a process divided into three steps: first of all we derived a meteorological scenario from one or more radar measurements; after that we conducted a simulation over this synthetic environment, imposing in the simulation all the radar parameters of the related measurement. Lastly, we compared the simulated radar measurables with the observed ones, aiming at similar results in a statistical sense. Validations have been carried out both on small scale and large scale, depending on the size of the meteorological scenario over which the simulation was performed.

6.1 Validations over small scale

The small scale validations were performed over very small environments, at the limit made by only one radar cell. For these simulations our goal was to obtain very accurate and detailed results. In order to perform these validations has been extremely helpful to use the measurements acquired from Vercelli with a PPI scan with almost vertical elevation. The parameters of the measurement follow: number of transmitted pulses=6800, PRF=1200 Hz, PW=1 μs, range resolution Δr=41.7 m, elevation θ=89.5°, azimuth scan from -85° to 175°. In this way it was possible to get the vertical profile of reflectivity, where can be clearly recognized different types of hydrometeors, such as the rain, the melting layer and the ice.

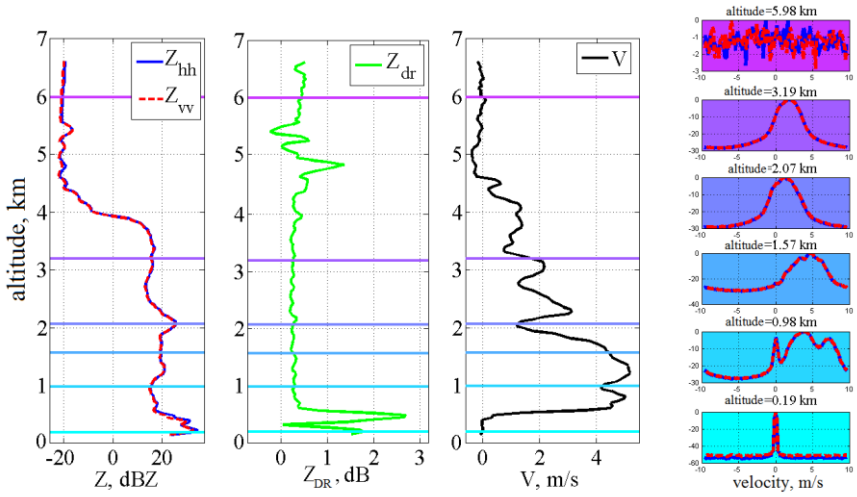

Figure 7: Vertical profile of Z_h, Z_v, Z_{DR}, V and Doppler spectra at six altitudes (blue indicates the horizontal polarization, red the vertical one) measured in Vercelli. Date is 15-October-2012, and time 14:57 UTC.

From the profile of Z can be easily seen the peak of the melting layer, a region which extends for about 350 meters from the 0˚C isotherm, located at an altitude of 2200 meters. Moreover, below the melting layer there is a rainy region with a quite flat reflectivity profile, while at heights above the 0˚C isotherm there is the presence of ice. On the contrary, the profile Z_{DR} is close to zero, because the antenna is rotating over the azimuth during the scan. The Doppler spectra estimated at six different altitudes are depicted in Fig. 7 on the right. From the bottom to the top, they refer respectively to the clutter, the rain (with and without clutter), the peak of the melting layer, the ice and finally to the background noise (which is almost white). The purpose of these validations was to reproduce with CleoSim the measured reflectivity and spectrum, simulating independently rain, melting layer and ice.

6.1.1 Rain

The rain measured at the altitude of 1400 meters has a reflectivity of 19.5 dBZ. From this value was derived the water content W to be placed in the meteorological grid. The conversion Z-W has been done using the same microphysical models implemented in CleoSim (Ulbrich, 1983). Such simulation has produced Z=20.6 dBZ (1 dB discrepancy) and a Doppler spectrum with significant similarities with the measured one. Furthermore, by applying to the simulation an updraft with an intensity of 0.7 m/s, which is potentially present in the measurement, the comparison becomes remarkable (as shown in Fig 8).

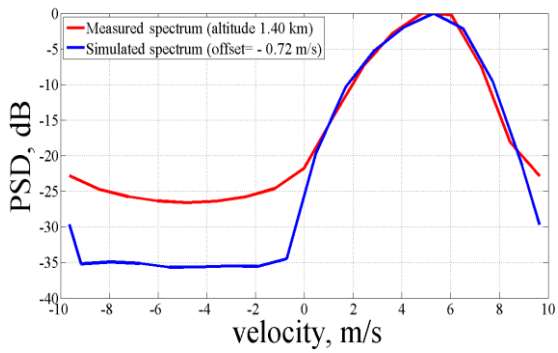

Figure 8: Simulated Doppler spectrum (with downdraft of 0.72 m/s) and measured Doppler spectrum by Vercelli radar at the altitude of 1400 m on October 26, 2012 at 14:57.

6.1.2 Melting Layer

The measured reflectivity profile of the melting layer, which can be seen in Fig. 9 (on the left), is characterized by a peak enhancement of about 6 dB over a rainy region with Z=19.5 dBZ. In order to simulate the melting layer CleoSim requires two parameters, namely the water content W of the rainy region below the melting layer and the initial density δ of the melting particles. Then, the altitude of the 0˚C isotherm is also needed. For the following case study, we found $W=4\cdot10^{-5}$ kg/m^3 and δ=0.31 g/cm^3 (D'Amico et al., 1998). The results of the simulations, compared with the measured ones, are shown in Fig. 9 for Z, *v* and the Doppler spectrum (estimated at the peak of the melting layer). As already found for the rain, the measured and the simulated spectra show a good level of agreement assuming the presence of an updraft of 2.7 m/s.

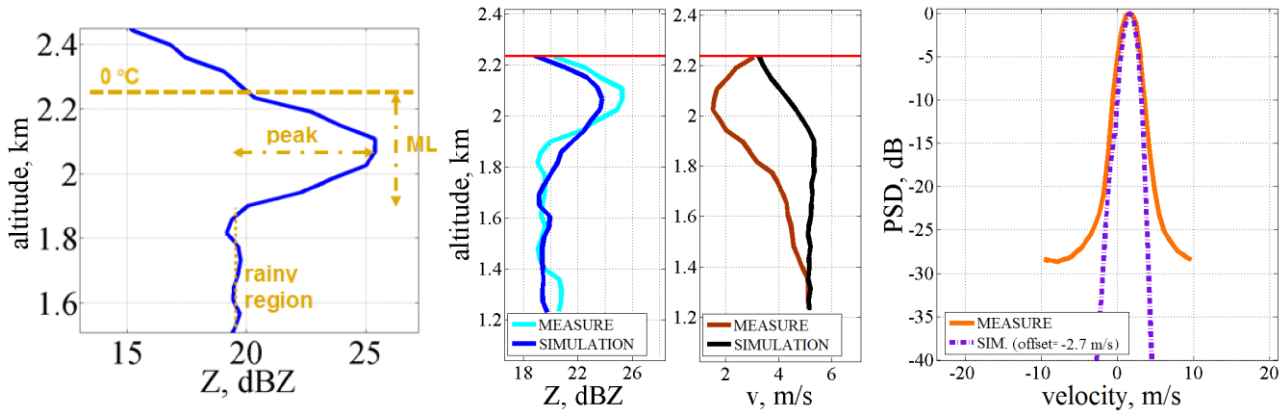

Figure 9: The first picture on the left is an enlargement of the melting layer region observed in the profile in Fig.7. The two figures in the middle show simulated and measured Z and Z_{DR} vertical profile along melting layer. On the right are showed the simulated and measured Doppler spectrum at the peak of melting layer.

6.1.3 Ice

The ice was detected around an altitude of 3200 meters, with a reflectivity of 15.5 dBZ. The meteorological parameters that feed the simulator are the temperature T at ice height and the ice water content IWC. The temperature has been easily estimated from the 0˚C isotherm (T≅ −6.5˚C), while we derived the IWC inverting the theoretical definition of Z, applying the Rayleigh approximation:

$$Z = \frac{1}{k}\cdot 10^6 \int_{D_{min}}^{D_{max}} N(D, IWC, T) D^6 dD \qquad (6.1)$$

where k=$|K_{water}|^2/|K_{ice}|^2 = 5.16$ is a constant which takes into account the disparity of the refractive index of ice from the refractive index of water, used to measure the reflectivity vertical profile (Fig. 7).

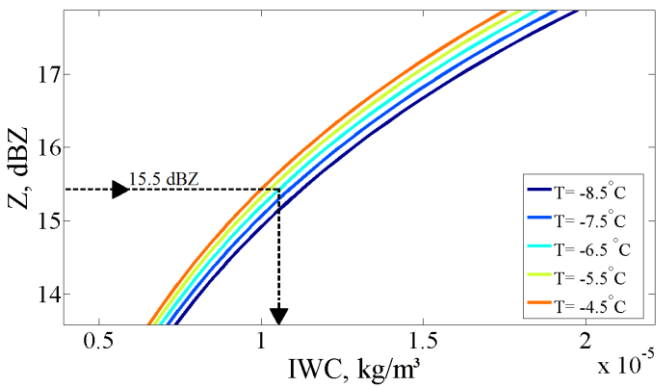

Figure 10: Relation between measured reflectivity in the "ice region" and IWC to feed CleoSim for different temperatures (ranging from -4.5˚C to -8.5˚C).

The simulated reflectivity was found equal to 13.02 dBZ. The discrepancy between the measured and simulated values can be explained with the uncertainties of the estimated temperature, which in turn affects the IWC estimation and the DSD, which depends on both temperature and ice water content. Further simulations have been performing to validate the Doppler spectrum of the ice crystals, as already done for raindrops and melting particles (Heymsfield et al., 2013).

6.2 Validations over large scale

The large scale validations were performed over a mesoscale meteorological environment: at this purpose was used the scenario between the two radars, to exploit images collocated and synchronous. It appears useful the possibility to use the RHI scans collected by the two radars, in order to work on the vertical plane that goes from Bric to Vercelli. As reported in Tab. 2, the RHI from Vercelli to Bric is available, but we don't have the opposite measurement, form Bric to Vercelli. So a "pseudo-RHI" from Bric had to be derived from the volumetric scan, performing the following steps:

a) From the volumetric scan of Bric we selected only the measurements acquired when the radar was pointing toward Vercelli (azimuth 61˚). In this way we derived 11 elevations.

b) We linearly interpolated these 11 elevations, that were limited and overturned, so to cover the entire angle between 0˚ and 28.5˚.

c) We can compare the measured RHI from Vercelli with the pseudo-RHI derived from the volumetric of Bric.

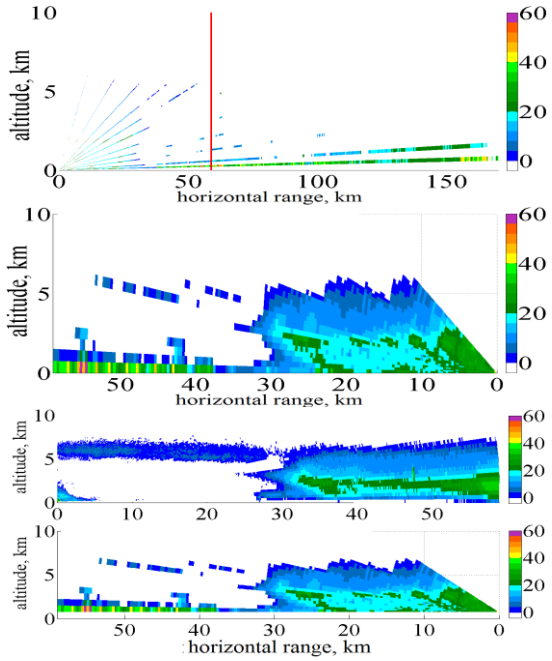

Figure 11: Steps of the algorithm to obtain a pseudo-RHI toward Vercelli from a volumetric scan of Bric. Date is 26-October-2012, and time 17:00 UTC.

In Fig. 12 are compared the RHI collected from Vercelli and the pseudo-RHI derived from Bric. The figures show a good level of agreement, even more so considering that the two radars work at different frequencies and the pseudo-RHI contains some lack of information.

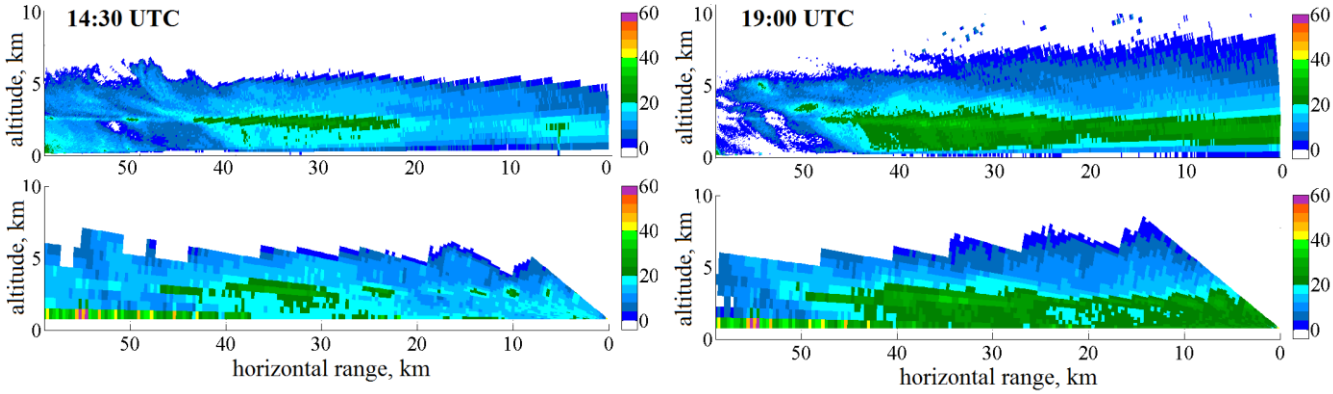

Figure 12: Comparison between co-located fields of reflectivity collected by means of RHI scans in Vercelli (figures on the top) and pseudo-RHI scans in Bric (figures on the bottom). Date is 26-October-2012, and time 14:30 UTC (on the left) and 19:00 UTC (on the right).

The radar measurable used to conduct the large scale validations is the field of reflectivity measured from the two radars on October 26, 2012 at 17:00 UTC (Fig. 11). In particular, the synthetic meteorological environment was derived from the pseudo-RHI of Bric calculated before, since this measurement is less affected by the attenuation. In this scenario we performed two simulations, the first from Bric perspective, the second from Vercelli one. Then, we compared the simulated field of Z with the measurement gathered by the respective radar.

The results of the two comparisons between measurement and simulation are depicted in the following figures. Note that the comparison conducted from Bric shows a better similarity because only one measurement was employed (Fig. 13 on the left). On the contrary, for the comparison from Vercelli we used two independent observations: we derived the meteorological environment from the pseudo-RHI from Bric, while we are comparing the simulation with the RHI form Vercelli. Although the two measurements employed were not perfectly identical (Fig. 11 on the bottom), we still find that the simulation is working properly (Fig. 13 on the right).

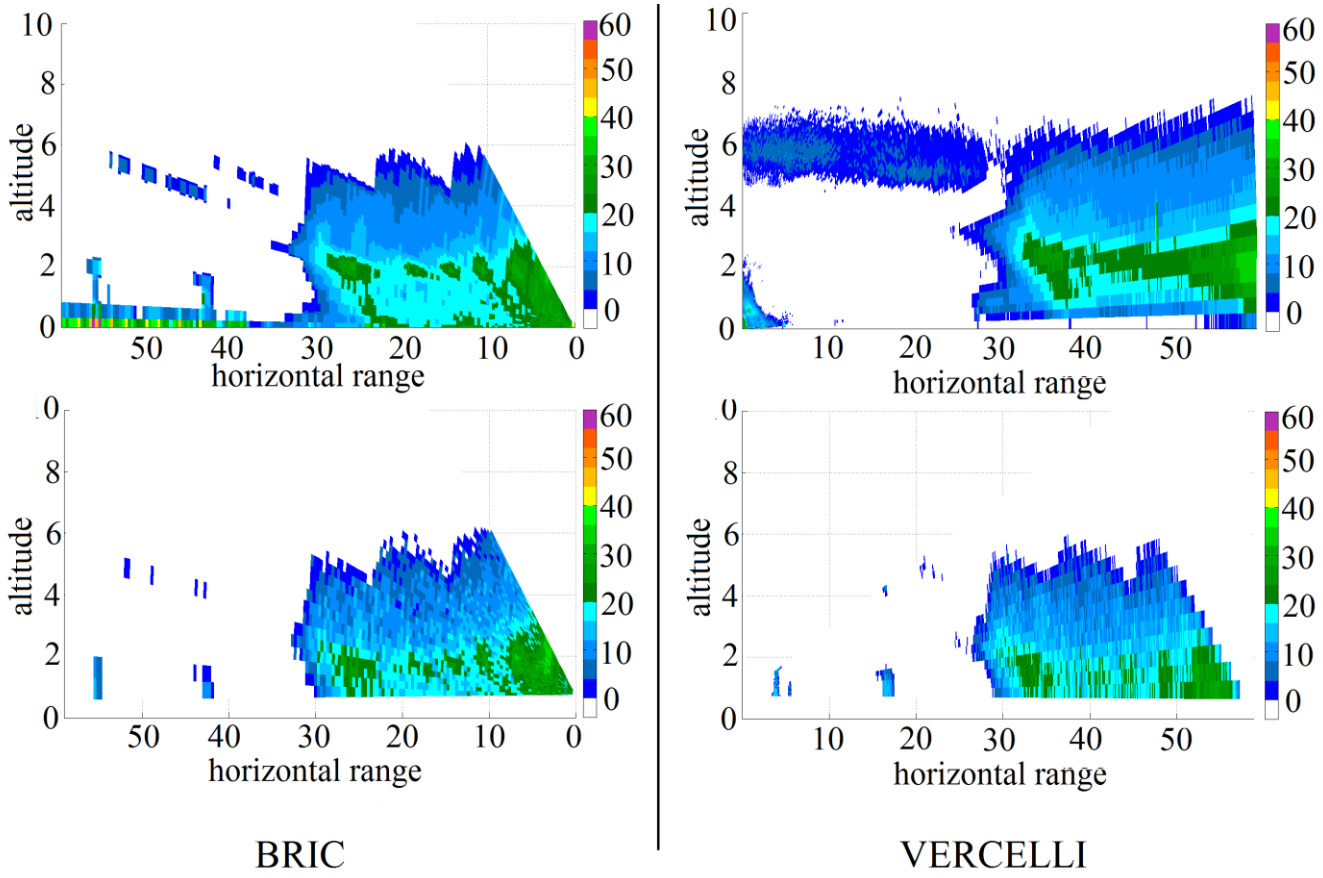

Figure 13: Results of validation process. On the left the validation conducted form Bric, on the right the validation form Vercelli. The measured fields of Z are on the top, while the simulated ones on the bottom.

7 Summary and outlook

In this contribution we presented the results of the main simulations that were conducted to validate the weather airborne simulator CleoSim, developed during the Cleopatra project. Both the simulations performed over analytic scenarios and those over environments derived from experimental observations have produced results coherent with the expectations. The measurements, gathered concurrently by two ground-based Doppler-polarimetric radars (operating at C and X band) operated by ARPAP, allowed us to validate CleoSim over small scale (simulating independently rain, melting layer and ice) and large scale environments. For the future, the validation of the simulator will continue during X-WALD project, where measurements will be collected with an airborne radar, in order to test the CleoSim performances over environments more suited to an airborne simulator.

Acknowledgement

This research has received funding from the European Union's Seventh Framework Programme (FP7/2007-2013) for the Clean Sky Joint Technology Initiative under grant agreement n. 271847. We are grateful to all people from IDS and ARPAP for overseeing the upgrade of the software and providing the data from the radars.

References

Doviak R.J. and D.S. Zrnić, Doppler Radar and Weather Observations. *San Diego, Academic Press, Inc.*, 1993. p. 562.

J.P. Wasselin, RT/2011/001, Cleopatra Project: State of the art of Airborne Weather Radar, 2012.

CleanSky JTI, Annual Implementation Plan 2014, CS-GB-2013-13-12 AIP, 2014. URL: http://www.cleansky.eu/content/homepage/reference-documents, pag 54.

Capsoni, C., M. D'Amico, and R. Nebuloni, A Multiparameter Polarimetric Radar Simulator. *Journal of Atmospheric and Oceanic Technology*, 2001. 18(11): p. 1799-1809.

Battan L.J., Radar Observation of the Atmosphere, The University of Chicago Press, 1973. p. 324.

Ulbrich, C.W., Natural Variations in the Analytical Form of the Raindrop Size Distribution. Journal of *Climate and Applied Meteorology*, 1983. 22(10): p. 1764-1775.

D'Amico, M., Dual polarization, frequency agile radar investigated using new radar simulator. *Electronics Letters*, 1999. 35(4): p. 335-336.

Oguchi, T., Electromagnetic wave propagation and scattering in rain and other hydrometeors. *Proceedings of the IEEE*, 1983. 71(9): p. 1029-1078.

D'Amico, M., A.R. Holt, and C. Capsoni, An anisotropic model of the melting layer. *Radio Science*, 1998. 33(3): p. 535-552.

Heymsfield, A.J., C. Schmitt, A. Bansemer, Ice cloud particle size distributions and pressure-dependent terminal velocities from in situ observations at temperatures from 0 to -86. *J. Atmos. Sci.*, 2013, 70: p. 4123–4154.